A Journal of the Gesellschaft Deutscher Chemiker
Angewandte Chemie
GDCh
International Edition
www.angewandte.org

Title: Material-Efficient Microfluidic Platform for Exploratory Studies of Visible-Light Photoredox Catalysis

Authors: Connor W Coley, Milad Abolhasani, Hongkun Lin, and Klavs F. Jensen

To be cited as: *Angew. Chem. Int. Ed.* 10.1002/anie.201705148
Angew. Chem. 10.1002/ange.201705148

Link to VoR: http://dx.doi.org/10.1002/anie.201705148
http://dx.doi.org/10.1002/ange.201705148

WILEY-VCH

Material-Efficient Microfluidic Platform for Exploratory Studies of Visible-Light Photoredox Catalysis

Connor W. Coley[a], Milad Abolhasani[a, b], Hongkun Lin[a], and Klavs F. Jensen*[a]

Abstract: We present an automated microfluidic platform for in-flow studies of visible-light photoredox catalysis in liquid or gas-liquid reactions at the 15 μL scale. An oscillatory flow strategy enables flexible residence time while preserving the mixing and heat transfer advantages of flow systems. The adjustable photon flux possible with the platform is characterized using actinometry. Case studies of oxidative hydroxylation of phenylboronic acids and dimerization of thiophenol demonstrate the capabilities and advantages of the system. Reaction conditions identified through droplet screening translate directly to continuous synthesis with minor platform modifications.

Photoredox catalysis has rapidly grown as an attractive tool in organic synthesis. Reactions which might otherwise require harsh conditions (e.g., high temperatures, highly-reactive reagents) are successfully performed under ambient conditions using visible light to initiate photocatalyst-mediated electron transfer.[1] The relatively high absorption of organometallic complexes within the visible spectrum provides greater opportunity for selective photochemical transformations compared to direct use of light itself (i.e., UV irradiation).[1d, 2] The redox process, owing to the long-lived photoexcited state of the activated photocatalyst, enables a safer, cleaner, and more environmentally-friendly approach to organic synthesis.[1c]

In a typical experimental set-up for a photochemical reaction, a high-powered light source is placed next to the reaction vessel (Figure 1a). The vessel headspace may be pressurized to increase the gas solubility and accelerate the gas-liquid reaction. Despite the prevalence of batch processes, they are often time- and labor-intensive to set up and do not provide precise control over reaction conditions. For example, strong visible-light irradiation can heat reaction mixtures, leading to an unknown increase in the reaction temperature, thereby making it challenging to decouple the effects of heat and photocatalyst activation. Moreover, the exponential decay of light intensity with penetration depth results in only partial activation of the available photocatalyst within the reaction vessel at each moment in time, necessitating reaction timescales on the order of hours to days.

Flow chemistry has addressed the aforementioned limitations of batch photochemical reactors by reducing the characteristic reaction vessel length scale from centimeters to hundreds of micrometers.[3] Small-scale continuous flow reactors (Figure 1b) typically use small inner diameter transparent tubing (ca. 1/16 or 1/32 in.) coiled around a light source. The small length scale significantly enhances the absorbed photon flux and gas-liquid mass transfer.[4] Nevertheless, the milliliter-scale reagent volumes required per reaction condition make it challenging to apply continuous flow chemistry approaches to the screening, characterization, optimization, and development of photocatalytic reactions.[4f]

In this study, building off our previous work with single-droplet oscillatory flow reactors,[5] we report an automated platform designed for screening and optimization of photocatalyzed liquid or gas-liquid reactions (Figure 1c). Microreaction vessels (i.e., droplets) of 15 μL are prepared on-demand by a computer-controlled liquid handler, injected into the system flowpath, and moved within gas-filled fluoropolymer tubing to a horseshoe-shaped photoreactor zone; the optically transparent reactor is illuminated from the top using a high intensity LED integrated via a custom-designed aluminum chuck. The reactor housing is mounted on a thermoelectric plate for active temperature control. Constant oscillatory motion of the droplet within the photoreactor promotes gas/liquid mass transfer and ensures that the reaction mixture remains well-mixed over the course of the reaction. After the desired reaction time, a sample of the crude product mixture (1-6 μL) is automatically injected into an LC/MS unit for analysis.

The modular platform offers some distinct advantages over traditional continuous flow techniques. Oscillatory motion within the reactor enables a wide range of residence times and decouples reaction time and mass transfer rates (i.e., via linear velocity). The carrier gas phase is easily reconfigurable between reactive gases (e.g., oxygen) and inert gases (e.g., argon) depending on the particular chemistry being studied. In addition, the carrier gas pressure, P_G, can be adjusted (0 - 2 MPa) to study its effect on reaction kinetics. Furthermore, the system can be reconfigured from discrete screening (oscillatory flow) to production (continuous flow) under identical reaction conditions.

To better understand the irradiation characteristics of the oscillatory flow platform, actinometry was used to quantify the photon flux in the reactor. The absorbed photon flux (photons per unit time) can be calculated from the rate of reaction (molecules consumed per unit time) normalized by the reaction's known quantum yield. Here, we use the aerobic oxidation of 9,10-diphenylanthracene (**1**, DPA) to the peroxide **2** in the presence of $Ru(bpy)_3Cl_2$, shown in Scheme 1a. [6]

Figure 2 shows the results of the actinometry experiments. Using a fiber-coupled broad spectrum light source and UV-Vis spectrometer at the optical detection point (Figure 2a), the absorbance spectrum of the reaction mixture is obtained in real-time (Figure 2b). Monitoring DPA absorbance at 372 nm under different irradiation intensities as measured by LED input power (Figure 2c) in combination with fitted first-order rate coefficients allow the calculation of absorbed photon flux. For example, at 400 mW, the absorbed photon flux is ~ 3×10^{-10} mol hv/s, or 2×10^{-2} mol hv/m^3/s (Figure 2d).

---

[a] C. W. Coley, Dr. M. Abolhasani, Dr. H. Lin, Prof. K. F. Jensen
Department of Chemical Engineering
Massachusetts Institute of Technology
77 Massachsuetts Avenue, Cambridge, MA 02139
E-mail: kfjensen@mit.edu
[b] Department of Chemical and Biomolecular Engineering
North Carolina State University
911 Partners Way, Raleigh, NC 27695

Supporting information for this article is given via a link at the end of the document.

10.1002/anie.201705148

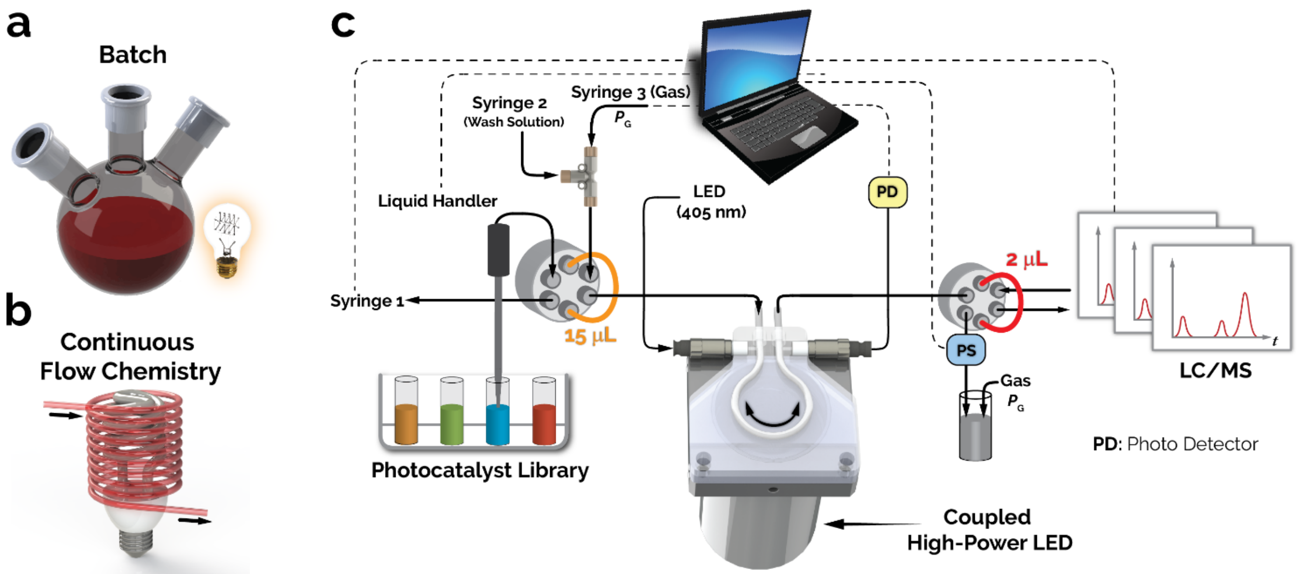

Figure 1. Schematics of traditional (a) batch and (b) continuous flow strategies for photochemical synthesis. (c) The experimental setup developed for single droplet studies of visible-light photoredox catalysis using an oscillatory flow strategy.

To demonstrate the versatility and efficacy of the developed flow chemistry platform for in-flow studies of visible-light photocatalyzed reactions, we first consider the oxidative hydroxylation of arylboronic acids to their corresponding phenols. Phenols are prevalent in biologically active compounds and small-molecule drugs, but their late-stage synthesis through traditional nucleophilic substitution can be challenging due to functional group incompatibilities and generation of side products.[7] Among the many approaches to this transformation, Zou et al.[8] have reported the use of $Ru(bpy)_3Cl_2$ as a photocatalyst to generate radical oxygen anion $O_2^{\bullet-}$ *in situ*, which readily reacts at the boron center (Figure 3a). Despite achieving high yields (71-96%), the use of batch vessels and need for long reaction times (16-72 hours) are obstacles to translating this approach to the production scale. We thus apply our flow chemistry platform to study this reaction, for the first time, under conditions one might employ for continuous flow synthesis to convert various phenylboronic acids (**3**) to the corresponding phenols (**4**), shown in Scheme 1b.

An initial screening of LED photon fluxes at fixed residence times of 3.6 and 25 minutes for phenylboronic acid is shown in Figure 3b. At low residence times, higher light intensity is always preferred; however, at longer residence times, an internal optimum at 6 W is observed. Figure 3c corroborates this trade-off via the time evolution of phenol yield at the optimum (6 W) and maximum (37 W) LED input powers. The apparent zeroth order kinetics with respect to **3** at 6 W demonstrates that the photocatalytic cycle is initially rate-limiting at this low input power (Figure 3c inset).

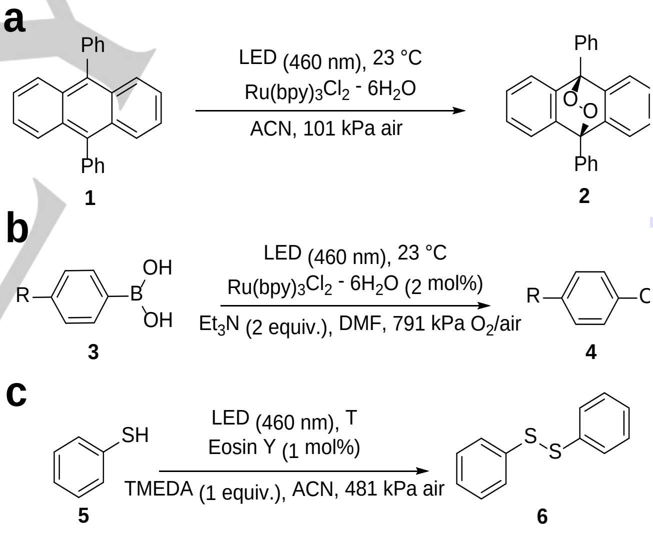

Scheme 1. Representative visible-light photocatalyzed reactions. (a) Oxidation of 9,10-diphenylathracene as a chemical actinometer; (b) oxidative hydroxylation of phenylboronic acids; (c) dimerization of thiophenol to diphenyldisulfide.

10.1002/anie.201705148

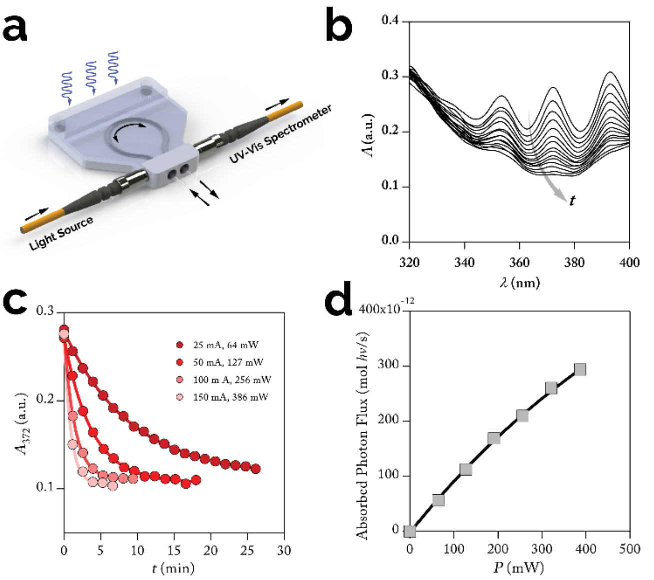

Figure 2. (a) Modified oscillatory photochemical reactor for *in-situ* actinometry measurements; (b) time evolution of the UV absorption spectra of the reaction mixture during oxidation of **1**; (c) decay in the absorbance of **1** at 372 nm under different irradiation conditions; (d) calculated absorbed photon flux at different LED powers.

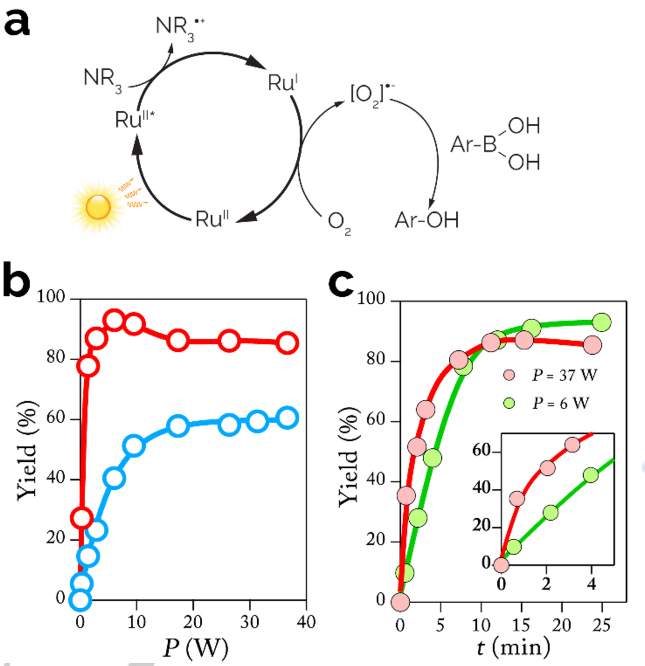

Figure 3. (a) Mechanism of the photocatalyzed oxidative hydroxylation of arylboronic acids, reproduced from [8]; (b) screening of LED currents at fixed residence times of 3.6 minutes (blue) and 25 minutes (red) for the oxidation of **3** (R=H); (c) time evolution of phenol yield under two LED powers.

To better understand this phenomenon, additional substrates (**3**, R = Me, Et, MeO, F, CN, Cl) were studied under similar conditions. The maximum yields observed for each substrate are summarized in Table S1. Time studies of the selected substrates at 6 W and 37 W are shown in Figure 4ab and 4cd. Compared to the previously-reported batch reaction,[8] reaction times using our developed flow chemistry platform are substantially reduced (e.g., 16 hours versus 10 minutes for R = CN). However, as shown in Figure 4, yields of product **4** for the ethyl, methyl, methoxy, and fluoro substrates exhibit a significant decrease with increasing residence time. The observed decrease in the reaction yield might be explained by the substantially higher oxygen pressure of our system (791 kPa O_2 versus 21 kPa O_2 in Zou et al.[8]) and the enhanced photon flux, both contributing to over-oxidation of the phenolic product. All substrates reached near 100% conversion.

The observed over-oxidation tendency is most pronounced for the methoxy, methyl, ethyl, and fluoro substrates, but also occurs in the cyano and chloro substrates. Online LC/MS analysis reveals the emergence of an over-oxidized side product in all cases except R = H. The observed trend is consistent with classic Hammet substituent effects, which capture a combination of inductive and resonance effects (Table S3).[9]

The aluminum housing of the Teflon reactor in combination with a thermoelectric plate allows for an accurate and systematic study of the effect of reaction temperature, without the typical confounding heating that results at high LED powers. This ability is demonstrated via the photocatalytic oxidation of thiophenol (**5**) to diphenyldisulfide (**6**) (Scheme 1c). This photo-oxidation reaction is an attractive means of accessing disulfide compounds, previously demonstrated in both batch and flow.[4e, 10] Understanding of and control over the formation of disulfide bridges are essential to realize protein folding[11] and synthesize protein analogues.[12] As shown in Figure 5bc, high conversions of **5** to **6** was achieved in short reaction times, even at very low LED powers of 38 and 64 mW. At higher powers of 2.8 and 37 W, conversion is completed within 2 minutes at 23 °C and within 1 minute at 35 °C. The enhanced reaction rate is directly associated with the effect of the increased temperature.

The modularity of the designed flow chemistry platform makes it adaptable to continuous organic synthesis (Section S5). The reaction in Scheme 1c was conducted at 35 °C using a total volumetric flow rate of 250 µL/min, providing an irradiation time of 50 s. Crude reaction mixtures were collected over 30 minutes of operation and showed complete conversion to **6** with a gas:liquid ratio of 4:1 at 2.8 W and 37 W and a conversion of 99% with 2:1 at 37 W. The direct translatability of conditions from screening to continuous synthesis without any measurable loss in performance further demonstrates the unique advantages of this platform, enabling simultaneous reaction discovery and optimization as well as continuous scaled-up synthesis.

In conclusion, the reported experimental setup enables material efficient screening and optimization of continuous (e.g., reaction time, LED power, temperature) and discrete (e.g., substrates) parameters associated with photocatalyzed reactions using only 30 µL of the reaction mixture per experimental condition (30 µL prepared, 15 µL injected). 150 reaction conditions were explored using a total volume of only 4.5 mL. Screening results are readily translated to continuous synthesis at the same characteristic length scale and irradiation flux and could be scaled-out using multiple reactors.

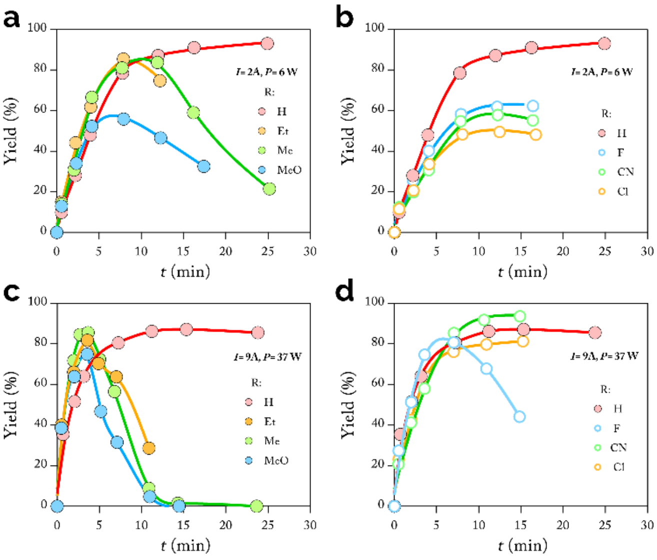

Figure 4. Yield of **4** as a function of time for (a,c) electron-donating and (b,d) electron-withdrawing substrates with operating under an LED power of (a, b) 6 W and (c, d) 37 W. Individual experiments are tabulated in Table S2. Gas: 791 kPa O_2.

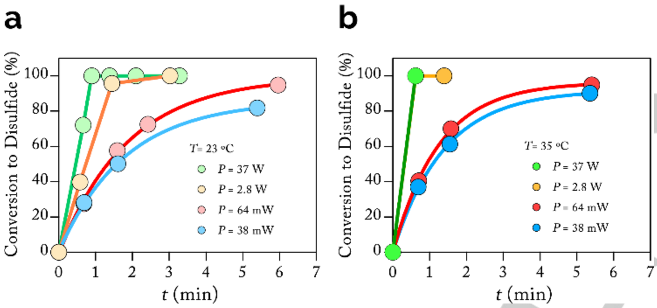

Figure 5. Effect of temperature and LED power on the photocatalytic dimerization of **5**. Gas: 481 kPa air.

Acknowledgements

We thank the Novartis Center for Continuous Manufacturing for funding this research. C.W.C. thanks the National Science Foundation Graduate Research Fellowship Program for support under Grant No. 1122374.

Keywords: photocatalysis • microreactors • high-throughput screening • flow chemistry, droplet microfluidics

References

[1] a) J. M. R. Narayanam, C. R. J. Stephenson, *Chem. Soc. Rev.* **2011**, *40*, 102-113; b) J. Xuan, W.-J. Xiao, *Angew. Chem. Int. Ed.* **2012**, *51*, 6828-6838; c) C. K. Prier, D. A. Rankic, D. W. MacMillan, *Chem. Rev.* **2013**, *113*, 5322-5363; d) T. P. Yoon, M. A. Ischay, J. Du, *Nat. Chem.* **2010**, *2*, 527-532; e) D. A. Nicewicz, D. W. MacMillan, *Science* **2008**, *322*, 77-80.

[2] K. Zeitler, *Angew. Chem. Int. Ed.* **2009**, *48*, 9785-9789.

[3] a) Y. Su, N. J. Straathof, V. Hessel, T. Noel, *Chem. Eur. J.* **2014**, *20*, 10562-10589; b) L. D. Elliott, J. P. Knowles, P. J. Koovits, K. G. Maskill, M. J. Ralph, G. Lejeune, L. J. Edwards, R. I. Robinson, I. R. Clemens, B. Cox, *Chem. Eur. J.* **2014**, *20*, 15226-15232; c) D. Cambié, C. Bottecchia, N. J. W. Straathof, V. Hessel, T. Noël, *Chem. Rev.* **2016**, *116*, 10276-10341; d) A. C. Hernandez - Perez, A. Caron, S. K. Collins, *Chem. Eur. J.* **2015**, *21*, 16673-16678.

[4] a) T. Aillet, K. Loubiere, O. Dechy-Cabaret, L. Prat, in *Int. J. Chem. React. Eng., Vol. 12*, **2014**, p. 257; b) J. P. Knowles, L. D. Elliott, K. I. Booker-Milburn, *Beilstein J. Org. Chem.* **2012**, *8*, 2025-2052; c) Z. J. Garlets, J. D. Nguyen, C. R. J. Stephenson, *Isr. J. Chem.* **2014**, *54*, 351-360; d) J. W. Tucker, Y. Zhang, T. F. Jamison, C. R. J. Stephenson, *Angew. Chem. Int. Ed.* **2012**, *51*, 4144-4147; e) Y. Su, V. Hessel, T. Noël, *AIChE J.* **2015**, *61*, 2215-2227; f) D. K. B. Mohamed, X. Yu, J. Li, J. Wu, *Tetrahedron Lett.* **2016**, *57*, 3965-3977; g) V. I. Martin, J. R. Goodell, O. J. Ingham, J. A. Porco, A. B. Beeler, *J. Org. Chem.* **2014**, *79*, 3838-3846; h) J. D. Nguyen, B. Reiß, C. Dai, C. R. Stephenson, *Chem. Commun.* **2013**, *49*, 4352-4354.

[5] a) M. Abolhasani, C. W. Coley, L. Xie, O. Chen, M. G. Bawendi, K. F. Jensen, *Chem. Mater.* **2015**, *27*, 6131-6138; b) M. Abolhasani, N. C. Bruno, K. F. Jensen, *Chem Comm* **2015**, *51*, 8916-8919; c) M. Abolhasani, K. F. Jensen, *Lab. Chip* **2016**, *16*, 2775-2784; d) Y.-J. Hwang, C. W. Coley, M. Abolhasani, A. Marzinzik, G. Koch, C. Spanka, H. Lehmann, K. F. Jensen, *Chem. Commun.* **2017**.

[6] S. P. Pitre, C. D. McTiernan, W. Vine, R. DiPucchio, M. Grenier, J. C. Scaiano, *Scientific reports* **2015**, *5*.

[7] C. González, L. Castedo, in *PATAI'S Chemistry of Functional Groups*, John Wiley & Sons, Ltd, **2009**.

[8] Y. Q. Zou, J. R. Chen, X. P. Liu, L. Q. Lu, R. L. Davis, K. A. Jørgensen, W. J. Xiao, *Angew. Chem.* **2012**, *124*, 808-812.

[9] L. P. Hammett, *J. Am. Chem. Soc.* **1937**, *59*, 96-103.

[10] Y. Su, A. Talla, V. Hessel, T. Noël, *Chem. Eng. Technol.* **2015**, *38*, 1733-1742.

[11] a) W. J. Wedemeyer, E. Welker, M. Narayan, H. A. Scheraga, *Biochemistry* **2000**, *39*, 4207-4216; b) A. McAuley, J. Jacob, C. G. Kolvenbach, K. Westland, H. J. Lee, S. R. Brych, D. Rehder, G. R. Kleemann, D. N. Brems, M. Matsumura, *Protein Sci.* **2008**, *17*, 95-106.

[12] a) S. B. Kent, *Chem. Soc. Rev.* **2009**, *38*, 338-351; b) O. Hartley, H. Gaertner, J. Wilken, D. Thompson, R. Fish, A. Ramos, C. Pastore, B. Dufour, F. Cerini, A. Melotti, *PNAS* **2004**, *101*, 16460-16465; c) D. Andreu, F. Albericio, N. A. Solé, M. C. Munson, M. Ferrer, G. Barany, *Peptide synthesis protocols* **1995**, 91-169.